Biochimie 144 (2018) 63–73

Contents lists available at ScienceDirect

Biochimie

journal homepage: www.elsevier.com/locate/biochi

Research paper

Biochemical and structural characterization of *Marinomonas mediterranea* D-mannose isomerase Marme_2490 phylogenetically distant from known enzymes

Wataru Saburi [a, 1], Nongluck Jaito [a, 1], Koji Kato [b], Yuka Tanaka [a], Min Yao [b], Haruhide Mori [a, *]

[a] Research Faculty of Agriculture, Hokkaido University, N-9, W-9, Sapporo 060-8589, Japan
[b] Faculty of Advanced Life Science, Hokkaido University, N-10, W-8, Sapporo 060-0810, Japan

ARTICLE INFO

Article history:
Received 7 August 2017
Accepted 21 October 2017
Available online 26 October 2017

Keywords:
D-mannose isomerase
N-acylglucosamine 2-epimerase
Cellobiose 2-epimerase
Aldose-ketose isomerase
Isomerization

ABSTRACT

D-Mannose isomerase (MI) reversibly isomerizes D-mannose to D-fructose, and is attractive for producing D-mannose from inexpensive D-fructose. It belongs to the *N*-acylglucosamine 2-epimerase (AGE) superfamily along with AGE, cellobiose 2-epimerase (CE), and aldose-ketose isomerase (AKI). In this study, *Marinomonas mediterranea* Marme_2490, showing low sequence identity with any known enzymes, was found to isomerize D-mannose as its primary substrate. Marme_2490 also isomerized D-lyxose and 4-OH D-mannose derivatives (D-talose and 4-*O*-monosaccharyl-D-mannose). Its activity for D-lyxose is known in other D-mannose isomerizing enzymes, such as MI and AKI, but we identified, for the first time, its activity for 4-OH D-mannose derivatives. Marme_2490 did not isomerize D-glucose, as known MIs do not, while AKI isomerizes both D-mannose and D-glucose. Thus, Marme_2490 was concluded to be an MI.

The initial and equilibrium reaction products were analyzed by NMR to illuminate mechanistic information regarding the Marme_2490 reaction. The analysis of the initial reaction product revealed that β-D-mannose was formed. In the analysis of the equilibrated reaction products in D_2O, signals of 2-H of D-mannose and 1-H of D-fructose were clearly detected. This indicates that these protons are not substituted with deuterium from D_2O and Marme_2490 catalyzes the intramolecular proton transfer between 1-C and 2-C.

The crystal structure of Marme_2490 in a ligand-free form was determined and found that Marme_2490 is formed by an $(\alpha/\alpha)_6$-barrel, which is commonly observed in AGE superfamily enzymes. Despite diverse reaction specificities, the orientations of residues involved in catalysis and substrate binding by Marme_2490 were similar to those in both AKI (*Salmonella enterica* AKI) and epimerase (*Rhodothermus marinus* CE). The Marme_2490 structure suggested that the α7→α8 and α11→α12 loops of the catalytic domain participated in the formation of an open substrate-binding site to provide sufficient space to bind 4-OH D-mannose derivatives.

1. Introduction

Carbohydrate isomerases and epimerases catalyze the epimerization (interconversion of epimers) and isomerization (interconversion between aldose and ketose) of carbohydrates, respectively, and are essential in carbohydrate metabolism processes, such as glycolysis, the oxidative/reductive pentose phosphate pathways and the Leloir pathway. These enzymes are very useful in enzymatic carbohydrate conversions in industry. D-Xylose isomerase (EC 5.3.1.5), isomerizing D-glucose to D-fructose, is widely used to

Abbreviations: AGE, *N*-acylglucosamine 2-epimerase; AKI, aldose-ketose isomerase; CE, cellobiose 2-epimerase; EcAKI, *Escherichia coli* AKI; ESI-MS, electron spray ionization mass spectrometry; Glcβ1-4Man, β-D-glucopyranosyl-(1→4)-D-mannose; HSQC, heteronuclear single quantum correlation; MI, D-mannose isomerase; NMR, nuclear magnetic resonance; SeAKI, *Salmonella enterica* AKI; TfMI, *Thermobifida fusca* mannose isomerase; XfAGE, putative AGE from *Xylella fastidiosa*.

* Corresponding author.
E-mail address: hmori@chem.agr.hokudai.ac.jp (H. Mori).

[1] These authors contributed equally to this work.

https://doi.org/10.1016/j.biochi.2017.10.016
0300-9084/

produce the D-fructose-rich syrup [1] and facilitates biofuel production from lignocellulosic biomass [2]. Cellobiose 2-epimerase (CE; EC 5.1.3.11) and D-tagatose 3-epimerase (EC 5.1.3.31) are useful for the efficient productions of functional carbohydrates, epilactose [β-D-galactopyranosyl-(1→4)-D-mannose] and D-psicose, respectively [3,4].

D-Mannose isomerase (EC 5.3.1.7, MI) is a carbohydrate isomerase catalyzing the reversible isomerization of D-mannose to D-fructose. This enzyme was first found in *Pseudomonas saccharophila* [5], and to date, enzymes from various bacterial species, including *Agrobacterium radiobacter* [6], *Mycobacterium smegmatis* [7], *Pseudomonas cepacia* [8], *Thermobifida fusca* [9], and *Xanthomonas rubrilineans* [10], have been enzymatically characterized. MI converts inexpensive D-fructose to D-mannose at a conversion rate of ~30%, and has great potential in industrial D-mannose production. Among the characterized MIs, only the amino acid sequence of *T. fusca* MI (TfMI) is available [9], which shows high sequence identity with YihS proteins, of the aldose-ketose isomerases (AKI), from *Escherichia coli* and *Salmonella enterica* at 41.5 and 42.8%, respectively. AKI catalyzes the interconversion of D-mannose, D-glucose, and D-fructose [11]. MI is distinguishable from AKI, because MI does not have detectable activity for D-glucose [5,6,9].

MI and AKI belong to the *N*-acylglucosamine 2-epimerase (AGE) superfamily together with carbohydrate epimerases: AGE (EC 5.1.3.8), epimerizing *N*-acetyl-D-glucosamine to *N*-acetyl-D-mannosamine, and CE, catalyzing the interconversion between reducing-end D-glucose and D-mannose residues of β-(1→4)-linked disaccharides. AGE superfamily enzymes share the $(\alpha/\alpha)_6$-barrel catalytic domain and several residues involved in catalysis and substrate binding (reducing-end sugar binding in CE) [11–15]. The mechanism of isomerization has been predicted based on the structure of *S. enterica* AKI (SeAKI) [11]; the catalytic His (His248 of SeAKI) abstracts the 2-H of D-mannose, to generate a *cis*-enediolate intermediate, and adds the proton to 1-C of the intermediate to produce D-fructose (Fig. 1A) [5]. Upon isomerization, the 1-O and 2-OH are protonated and deprotonated through an undetermined process, respectively. In contrast, in epimerizations catalyzed by AGE and CE, two catalytic His residues act as the general base and acid catalysts (Fig. 1B). The first catalytic His abstracts 2-H from the substrate, to generate the *cis*-enediolate intermediate, and the second catalytic His donates a proton to the intermediate, to produce the epimerized product [13–15].

The AGE superfamily includes many uncharacterized proteins

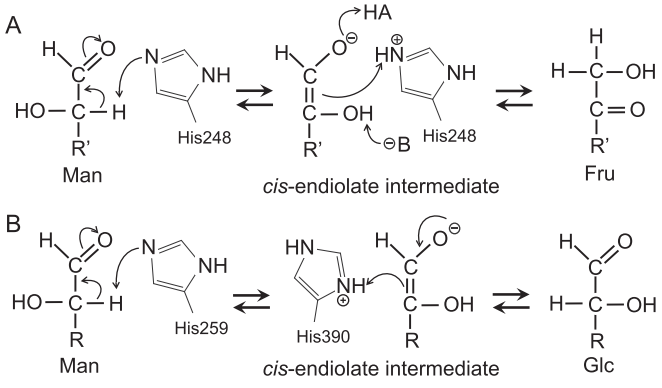

Fig. 1. Proposed reaction mechanisms of the isomerization and epimerization catalyzed by AGE superfamily enzymes. (A) Reaction mechanism of the isomerization. Amino acid numbering is for SeAKI. His248 abstracts 2-H of D-mannose and donates the proton to 1-C. Mechanisms of protonation of 1-O and deprotonation of 2-OH are unclear. (B) Reaction mechanism of the epimerization. Amino acid numbering is for RmCE. His259 abstracts 2-H from reducing end D-mannose residue, and His390 protonates the *cis*-enediolate intermediate to produce epimerized product.

that show low sequence similarity to any functionally known enzymes. Functional analysis of such uncharacterized proteins advances understanding the function-structure relationship of superfamily members. A putative AGE, Marme_2490 (GenBank number, ADZ91722.1) from a marine bacterium *M. mediterranea*, has only 13.7–25.1% sequence identity with any characterized AGE superfamily enzymes, and the function of this protein is as yet unknown. In this study, the characteristics of recombinant Marme_2490 produced in *Escherichia coli* were investigated and the results showed that this protein was not an AGE but an MI. Compared to other known MIs, Marme_2490 also possessed isomerization activity towards 4-OH derivatives of D-mannose (D-talose and 4-*O*-monosaccharyl-D-mannose). The three-dimensional structure of Marme_2490 in free form was analyzed, and the molecular basis for its substrate specificity discussed in structural comparison with other AGE superfamily enzymes.

2. Materials and methods

2.1. Production of recombinant Marme_2490 in E. coli

The gene encoding Marme_2490 was amplified by PCR. The genomic DNA of *M. mediterranea* NBRC 103028 (National Institute of Technology and Evaluation Biological Resource Center, Chiba, Japan) was used as the template. Primestar HS DNA polymerase (Takara Bio, Kusatsu, Japan) was used. Primers used in the PCR are as follows: 5′-AAAAAGAATTCATGTCTTACCCTGCATTTG-3′ (sense orientation, *Eco*RI site is underlined) and 5′-AAAAACTCGAG-TAAGGTCAGTGTTTTCAAT-3′ (antisense orientation, *Xho*I site is underlined). The PCR product was cloned into pET23a (Novagen, Darmstadt, Germany) using the restriction sites introduced. The DNA sequence of the inserted DNA including its flanking regions was determined using an Applied Biosystems 3130 Genetic Analyzer (Life Technologies, Carlsbad, CA, USA). Using this expression plasmid, in recombinant Marme_2490 produced, 16 amino acid residues (cloning artifact), Met-Ala-Ser-Met-Thr-Gly-Gly-Gln-Gln-Met-Gly-Arg-Gly-Ser-Glu-Phe, and 8 amino acid residues, Leu-Glu-His-His-His-His-His-His, were attached to the N and C-terminals of the registered amino acid sequence, respectively.

E. coli BL21 (DE3) transformants harboring the expression plasmid were cultured in 1 L of LB medium containing 50 μg/mL ampicillin at 37 °C. Protein expression was induced by the addition of 0.1 M isopropyl β-thiogalactopyranoside to a final concentration of 0.1 mM when the absorbance at 600 nm reached 0.6. The induction culture was carried out at 16 °C for 20 h. Bacterial cells were harvested by centrifugation at 8400 × *g* at 4 °C for 10 min, and resuspended in 40 mL of 20 mM sodium phosphate buffer containing 0.5 M NaCl (pH 7.0; buffer A). The cells were disrupted by sonication, and the cell debris was removed by centrifugation at 13,000 × *g* at 4 °C for 10 min. The cell-free extract obtained was applied onto a Ni-chelating Sepharose Fast Flow column (3.0 cm i.d. × 10.5 cm, GE Healthcare, Uppsala, Sweden), equilibrated with buffer A. The column was washed with buffer A containing 10 mM imidazole, and the adsorbed protein was eluted by a linear gradient of imidazole from 10 to 500 mM (total elution volume, 200 mL). The purity of the fraction was evaluated by SDS-PAGE. The fractions containing highly purified protein were collected and dialyzed against 10 mM sodium phosphate buffer (pH 7.0). The sample was concentrated to several mg/mL by ultrafiltration using Vivaspin 20 centrifugal concentrators (nominal molecular weight limit 30,000 Da; Sartorius, Göttingen, Germany) and stored at −20 °C in the presence of 50% glycerol. The concentration of the purified enzyme was calculated from the amino acid concentrations after complete acid hydrolysis using 6 M HCl. The amino acid concentrations were

measured by the ninhydrin colorimetric method [16].

2.2. Screening of substrate

The reaction mixture (25 μL) containing 40 mM sugar, 40 mM Tris-HCl buffer (pH 7.4) and 0.4 or 4.0 μM Marme_2490 was incubated at 30 °C for 10 min or 16 h. Following sugars are tested as candidate substrates: D-allose, 1,5-anhydro-D-glucitol, D-glucose, D-lyxose, D-mannose, methyl α-D-glucoside, methyl β-D-glucoside, D-tagatose, D-xylose (Wako Pure Chemical Industries, Osaka, Japan); D-altrose, cellobiose, 6-deoxy-D-glucose, D-mannose 6-phosphate, L-rhamnose, D-talose, D-xylulose (Sigma, St. Louis, MO, USA); D-fructose, D-galactose, D-glucitol, maltose, D-mannitol, *N*-acetyl-D-glucosamine (Nacalai Tesque, Kyoto, Japan); 2-deoxy-D-glucose (Tokyo Chemical Industry, Tokyo, Japan); D-arabinose, lactose, sucrose (Kanto Chemicals, Tokyo, Japan), epilactose [3], lactulose [β-D-galactopyranosyl-(1→4)-D-fructose; Acros Organics, Geel, Belgium], β-(1→4)-mannobiose [17], β-D-glucopyranosyl-(1→4)-D-mannose (Glcβ1-4Man) [18] and β-D-mannopyranosyl-(1→4)-D-glucose [17]. The reaction was terminated by heating at 100 °C for 3 min. The sample (1 μL) was spotted onto a silica gel plate (TLC Silica gel 60 F_{254} Aluminium sheet, 20 cm × 20 cm, Merck, Darmstadt, Germany) and developed twice by 2-propanol/1-butanol/water (2/2/1, v/v/v). Carbohydrates were detected by spraying a detection reagent [acetic acid/sulfuric acid/anisaldehyde (100/2/1, v/v/v)] onto the plate, followed by heating the plate.

2.3. Structural analysis of isomerized products from disaccharides

A reaction mixture (1 mL), containing 4.20–7.91 μM Marme_2490, 100 mM disaccharide (β-(1→4)-mannobiose, Glcβ1-4Man, or epilactose) and 40 mM Tris-HCl buffer (pH 7.4), was incubated at 30 °C for 24 h. The products were purified by TLC as described in section 2.2. One hundred microliter of the sample was applied per plate. The silica gel containing the product was scraped and suspended in 1 mL of distilled water to elute the reaction product. The gel was removed by centrifugation at 13,000 × *g* at 4 °C for 5 min. The supernatant was dried *in vacuo* at 40 °C. Chemical structures of the obtained products were analyzed by electron spray ionization mass spectrometry (ESI-MS) and nuclear magnetic resonance (NMR). ESI-MS was carried out with an Exactive mass spectrometer (Thermo Scientific, San Jose, CA, USA). The sample was subjected by flow injection. Methanol was used as the mobile phase solvent. The positive ion was detected under the following conditions: spray voltage, 3.00 kV; capillary temperature, 300 °C. NMR spectra were recorded in D_2O (Sigma) at 27 °C using a Bruker AMX500 (500 MHz; Bruker Corporation, Billerica, MA, USA). The chemical shifts in ^{13}C-NMR for the products from Glcβ1-4Man and epilactose were compared with those for cellobiulose [β-D-glucopyranosyl-(1→4)-D-fructose] and lactulose [19], respectively. A series of two-dimensional homo- and heteronuclear correlated spectra [correlated spectroscopy, heteronuclear single quantum correlation (HSQC), HSQC total correlation spectroscopy and heteronuclear multiple bond correlation correlated spectroscopy] were acquired to determine the chemical structure of the reaction product from β-(1→4)-mannobiose.

2.4. Enzyme assay

2.4.1. Standard enzyme assay

To determine isomerization activity against D-mannose, a reaction mixture (50 μL) containing 1–15 nM enzyme, 10 mM D-mannose, 40 mM Tris-HCl buffer (pH 7.4) and 0.02 mg/mL bovine serum albumin was incubated at 30 °C for 10 min. The reaction was stopped by heating at 100 °C for 3 min. The concentration of the produced D-fructose was measured using a D-fructose assay reagent (R-Biopharm AG, Darmstadt, Germany). Authentic D-fructose (0–2.5 mM) containing 10 mM D-mannose was used as the standard.

2.4.2. Effects of pH and temperature

The optimal pH was determined from the isomerization activity toward 10 mM D-mannose at various pH values. The enzyme assay was done under the conditions of the standard enzyme assay other than the reaction buffer. Sodium acetate buffer (pH 3.2–6.1), MES-NaOH buffer (pH 5.9–6.9), Tris-HCl buffer (pH 6.5–9.5) and Britton-Robinson buffer (pH 10.9–11.7) were used. The optimal temperature was examined by measuring enzyme activity at 10–50 °C. Stable ranges of pH and temperature were assessed by measuring residual activity after pH and temperature treatments. For the pH treatment, a mixture (50 μL) containing 20 μM Marme_2490 and 50 mM buffer described above (pH 3.2–11.7) was incubated at 4 °C for 24 h. For temperature treatment, a mixture (50 μL) containing 20 μM Marme_2490 and 10 mM Tris-HCl (pH 7.4) was incubated at 10–50 °C for 30 min. The range, in which the enzyme retained over 90% of the original activity, was regarded as the stable range.

2.4.3. Kinetic parameters for the isomerization

Kinetic parameters for the isomerization of D-mannose, D-talose and D-lyxose were determined from the reaction rates at various substrate concentrations. A reaction mixture (350 μL) containing 4.0–746 nM Marme_2490, 1–35 mM substrate, 40 mM Tris-HCl (pH 7.4) and 0.2 mg/mL bovine serum albumin was incubated at 30 °C. The reaction times for D-mannose, D-lyxose and D-talose were 15 min, 30 min and 6 h, respectively. Fifty micro-liters of the reaction mixture were taken every 3 min, 5 min and 1 h in the reaction with D-mannose, D-lyxose and D-talose, respectively. The reaction was stopped by heating the sample at 100 °C for 3 min. In the reaction with D-mannose, D-fructose produced was measured as described above. To determine the reaction rates for D-lyxose and D-talose, D-xylulose and D-tagatose were quantified, respectively, according to the colorimetric quantification method of ketoses [20]: the sample (50 μL) was mixed with 75 μL of 0.5 mg/mL resorcinol in ethanol and 75 μL of 0.216 g/L $FeNH_4(SO_4)_2 \cdot 12H_2O$ in HCl, and incubated at 80 °C for 40 min. The sample was cooled on ice, and the absorbance values at 480 nm and 640 nm of the resulting solutions were measured to determine D-xylulose and D-tagatose, respectively. As standards, 0–0.5 mM D-xylulose and 0–2.5 mM D-tagatose were used. Kinetic parameters were calculated by fitting the reaction velocities at various substrate concentrations to the Michaelis-Menten equation using Grafit version 7.0.2 (Erithacus Software, East Grinstead, UK).

2.4.4. Isomerization activity towards disaccharides

Isomerization activity to 100 mM β-(1→4)-mannobiose, epilactose, and Glcβ1-4Man were measured. A reaction mixture (1 mL), containing 5.12 μM Marme_2490, 100 mM substrate, 10 mM Tris-HCl buffer (pH 7.4), was incubated at 30 °C for 4 h. Aliquots (120 μL) were taken at 15, 30, 45, 60, 90, 120, 180, and 240 min, and heated in boiling water for 3 min to stop the reaction. Ten microliter of 130 mg/mL D-glucitol was added to the sample as internal standard, and the concentrations of the reaction products were determined by HPLC under following conditions: sample volume, 10 μL; column, HILIC Pak VG-50 4E (4.6 mm i.d. × 250 mm; Shodex, Tokyo, Japan); column temperature, 40 °C; eluent, acetonitrile/methanol/water (75/20/5, v/v/v); flow rate, 1 mL/min; detection, refractive index. Reaction velocity was calculated from the slope of the progress curve for the disaccharide isomerization.

2.4.5. Inhibition kinetics of inorganic phosphate

Inhibition kinetics of inorganic phosphate were carried out by

measuring the isomerization velocity to various concentrations of D-mannose in the absence and presence of 20 mM sodium phosphate (pH 7.4). The reaction rates obtained were fitted to the competitive inhibition equation using Grafit version 7.0.2, and the inhibition constant (K_i) of inorganic phosphate was determined.

2.5. Time course of the isomerization of D-mannose

A reaction mixture (375 μL) containing 1.28 μM Marme_2490, 10 mM D-mannose, and 40 mM Tris-HCl (pH 7.4) was incubated at 30 °C. Twenty-five μL samples were taken at indicated times and the reaction was terminated at 100 °C for 3 min. The D-fructose concentration produced was measured as described in section 2.4.1.

2.6. NMR analysis of reaction products

^{1}H-NMR was used to monitor the isomerization of D-fructose to D-mannose. H_2O in the Marme_2490 solution was replaced with D_2O: the enzyme solution was diluted 10-fold with 10 mM HEPES-Na buffer in D_2O (pD 7.8), and concentrated to the original volume by ultrafiltration, as described above. These steps were repeated three times in total. A reaction mixture (0.5 mL), containing 609 nM Marme_2490, 250 mM D-fructose and 10 mM HEPES-Na buffer (pD 7.8), was placed into an NMR tube, and immediately ^{1}H-NMR was recorded at 35 °C.

To obtain the reaction mixture that reached the equilibrium, the reaction mixture was incubated at room temperature for 24 h. The chemical structures of D-mannose and D-fructose in the mixture were analyzed by two-dimensional NMR as described above.

2.7. Measurement of the molecular mass of Marme_2490 under nondenaturing conditions

The molecular mass of Marme_2490 under nondenaturing conditions was measured by gel-filtration column chromatography under the following conditions: column, Asahipac GF-510 HQ (7.5 mm i.d. × 300 mm, Shodex); buffer, 10 mM Tris-HCl buffer containing 0.2 M NaCl (pH 7.0); flow rate, 0.5 mL/min; detection, absorbance at 280 nm. The Gel Filtration Standard (Bio-Rad, Hercules, CA, USA) containing a standard set of proteins was used to calibrate the gel-filtration column.

2.8. Crystallization and data collection of Marme_2490

Initial crystallization screening was performed using a series of crystallization kits from Qiagen (Hilden, Germany) by the sitting-drop vapor-diffusion method, in which 0.75 μL of 10 mg/mL protein solution in 10 mM Tris-HCl buffer (pH 7.4) was mixed with an equal volume of the reservoir solutions. The appropriate crystals of Marme_2490 were obtained within 1 month at 20 °C under the reservoir solution containing 80 mM sodium potassium phosphate, 0.1 M Bis Tris propane (pH 6.5) and 20% (w/v) PEG3350.

For X-ray diffraction experiments, the crystals of Marme_2490 were directly picked up from crystallization solution and flash cooled. Diffraction data were collected on beamline BL-44XU at SPring-8 (Hyogo, Japan), under a stream of liquid nitrogen at 100 K. The data set was indexed, integrated, scaled and merged using the XDS program suite [21]. The asymmetric unit of Marme_2490 contained two molecules corresponding to a Matthews coefficient [22] of 2.6 Å^3 Da^{-1} and an estimated solvent content of 52.8%. The data collection and processing statistics are summarized in Table 3.

2.9. Structure solution and refinement of Marme_2490

The structure of Marme_2490 was determined by the molecular replacement method with the program AutoMR in the Phenix program package [23,24], using the structure of acylglucosamine 2-epimerase (PDB ID: 3GT5) as the search model. Several rounds of refinement were performed using the program Phenix.refine in the Phenix program suite, alternating with manual fitting and rebuilding, based on 2Fo−Fc and Fo−Fc electron density using COOT [24,25]. The final refinement statistics and geometry defined by MolProbity [26] are shown in Table 3. All figures of structures were generated by the PyMol molecular graphics system version 1.7.4 (Schrödinger, LLC, New York, NY, USA).

3. Results

3.1. Substrate specificity

Recombinant Marme_2490 harboring a C-terminal His-tag was produced in *E. coli* BL21(DE3) cells. From the cell-free extract obtained from 1 L of the culture broth, recombinant Marme_2490 (19.4 mg) was purified to homogeneity by immobilized metal (Ni) affinity column chromatography. To screen substrates, the purified enzyme was incubated with various carbohydrates. Recombinant Marme_2490 (0.4 μM) converted D-mannose, D-fructose, D-lyxose and D-xylulose to D-fructose, D-mannose, D-xylulose and D-lyxose, respectively, in a 10 min reaction period (Fig. 2), indicating that Marme_2490 reversibly isomerized D-mannose and D-lyxose to the corresponding ketoses. In longer reaction (16 h) with a higher concentration of enzyme (4.0 μM), D-talose and D-tagatose were detected as the reaction products from D-tagatose and D-talose, respectively. The reaction products from β-(1→4)-mannobiose, epilactose, and Glcβ1-4Man were also detected. The chemical structures of the disaccharide products were analyzed by ESI-MS and NMR. The masses of all these disaccharide-products were 365.11 m/z $[M + Na]^+$. The chemical shifts in the ^{13}C-NMR for the products from epilactose and Glcβ1-4Man coincided with the reported values for lactulose and cellobiulose [19], respectively. The chemical structure of the reaction product from β-(1→4)-mannobiose was determined to be β-D-mannopyranosyl-(1→4)-D-fructose by two-dimensional NMR analysis (Table 1). The D-fructose residue adopted the β-D-fructopyranose- and β-D-fructofuranose-forms as the major and minor species, respectively, as judged from the signal intensity at 27 °C. No product was detected in the long-term reactions with D-allose, D-altrose, 1,5-anhydro-D-glucitol, D-arabinose, 2-deoxy-D-glucose, 6-deoxy-D-glucose, D-galactose, D-glucose, methyl α-D-glucopyranoside, methyl β-D-glucopyranoside, *N*-acetyl-D-glucosamine, L-rhamnose, sugar alcohols (D-glucitol and D-mannitol), sugar phosphate (D-mannose 6-phosphate) and following disaccharides: cellobiose, lactose, maltose, β-D-mannopyranosyl-(1→4)-D-glucose and sucrose.

3.2. Kinetic analysis of the isomerization catalyzed by Marme_2490

Marme_2490 showed the highest D-mannose-isomerizing activity at pH 7.3 and 30 °C. This enzyme was stable at 35 °C and lower (at pH 7.0 for 30 min), and in a pH range of 6.0–9.4 (4 °C for 24 h).

The kinetic parameters of Marme_2490 for D-mannose, D-lyxose and D-talose were determined (Table 2). Marme_2490 showed the highest k_{cat} and the lowest K_m values for D-mannose among these substrates. The k_{cat}/K_m value of Marme_2490 for D-mannose, 19.7 $s^{-1}mM^{-1}$, was 13- and 1700-fold higher than for D-lyxose and D-talose, respectively. Isomerization velocities to 100 mM disaccharide substrates, β-(1→4)-mannobiose, epilactose, and Glcβ1-4Man, were 0.0564 s^{-1}, 0.0987 s^{-1}, and 0.0890 s^{-1}, respectively, and are 0.020%, 0.035%, and 0.032% of the velocity to D-mannose at the same concentration, respectively. From these kinetic results, D-

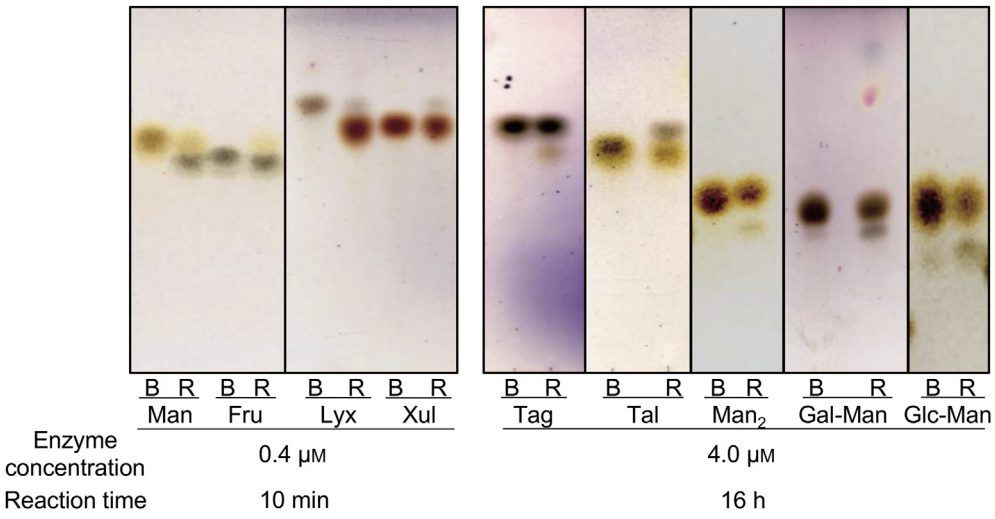

Fig. 2. TLC analysis of the reaction products of Marme_2490 from various substrates. Substrates are shown below the figure. Man_2, Gal-Man, and Glc-Man are β-(1→4)-mannobiose, epilactose and Glcβ1-4Man, respectively. Lanes B and R are the substrate solution and the reaction mixture after the reaction, respectively.

Table 1
Chemical shifts of the isomerized product from β-(1→4)-mannobiose.

β-D-Man*p*-(1→4)-β-D-Fru*p* (major)						β-D-Man*p*-(1→4)-β-D-Fru*f* (minor)				
residue	number	δ_C (ppm)	δ_H (ppm)	*J*H,H (Hz)		residue	number	δ_C (ppm)	δ_H (ppm)	*J*H,H (Hz)
β-Man	1	99.68*	4.87*	s		β-Man	1	102.56	4.77*	m
	2	73.64	4.07	brs			2	73.29	4.04	m
	3	75.67	3.68	m			3	75.55	3.66	m
	4	69.59	3.59	m			4	69.87	3.56	m
	5	79.14	3.40	dd	8.7, 8.1		5	78.93	3.44	m
	6	63.79	3.93	m			6	64.00	3.97	m
			3.74	m					3.71	m
β-Fru*p*	1	66.68	3.73	d	10.9	β-Fru*f*	1	65.47	3.61	m
			3.57	d	10.9				3.56	m
	2	100.80					2	105.26		
	3	68.85	3.93	d			3	77.54	4.28	m
	4	79.14*	4.16*	dd	9.4, 3.1		4	86.85*	4.27	m
	5	68.92	4.21	brs			5	82.80	4.00	m
	6	65.98	4.01	brd	12.9		6	65.35	3.78	m
			3.75	brd	12.9				3.71	m

s, singlet; brs, broad singlet; d, doublet; dd, double doublet; m, multiplet. *, correlation peak was observed in the heteronuclear multiple bond correlation spectrum.

Table 2
Kinetic parameters of Marme_2490 and other functionally related carbohydrate isomerases.

Enzyme	Reaction temperature (°C)	D-Mannose			D-Lyxose			D-Talose			Reference
		k_{cat} (s^{-1})	K_m (mM)	k_{cat}/K_m ($s^{-1}mM^{-1}$)	k_{cat} (s^{-1})	K_m (mM)	k_{cat}/K_m ($s^{-1}mM^{-1}$)	k_{cat} (s^{-1})	K_m (mM)	k_{cat}/K_m ($s^{-1}mM^{-1}$)	
Marme_2490	30	329 ± 2.2	16.7 ± 1.8	19.7	64.4 ± 3.6	42.3 ± 3.4	1.52	0.319 ± 0.05	27.8 ± 7.69	0.0115	This study
EcAKI	37	25.3 ± 1.0	108 ± 11	0.234	13.5 ± 0.6	405 ± 41.7	0.033	N.D.	N.D.	N.D.	[11]
SeAKI	37	23.3 ± 0.9	134 ± 15	0.174	N.D.	N.D.	N.D.	N.D.	N.D.	N.D.	[11]
TfMI	50	788 ± 40	115 ± 15	6.85	63.3 ± 6.5	537 ± 12	0.118	N.D.	N.D.	N.D.	[9]

Data are mean ± standard deviation for three independent experiments. N.D., not determined.

mannose is determined as the primary substrate of Marme_2490.

The isomerization of 10 mM D-mannose by Marme_2490 was monitored at 30 °C (Fig. 3). At reaction 80 min, the reaction reached the equilibrium, and D-fructose concentration was 6.98 mM, indicating 69.8% conversion of D-mannose. This result is consistent with the previously reported conversion levels, 65%–75%, obtained using MIs from *M. smegmatis*, *P. cepacia*, *T. fusca* and *X. rubrilineans* [7–10].

3.3. NMR analysis of the reaction product generated from D-fructose in D_2O

The isomerization of D-fructose to D-mannose by Marme_2490 was monitored by ^{1}H-NMR (Fig. 4A). During the initial stage of the reaction, the 1-H signal of β-D-mannose (4.92 ppm) was higher than that of α-D-mannose (5.18 ppm), which is more abundant than β-D-mannose in the equilibrium aqueous solution of D-mannose.

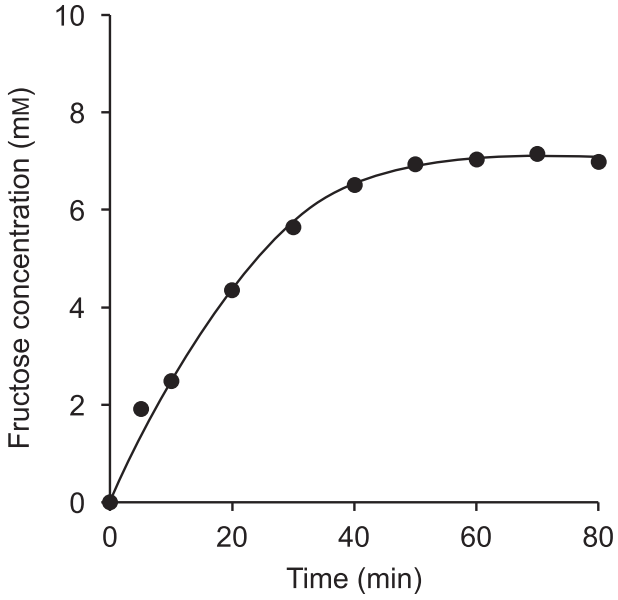

Fig. 3. Time course of isomerization of D-mannose. Isomerization of 10 mM D-mannose was monitored by measuring the concentration of D-fructose produced.

This result suggests that Marme_2490 produced β-D-mannose from D-fructose. The signal representing α-D-mannose increased at a later stage of the reaction.

After incubating the reaction mixture at room temperature for 24 h to prepare the equilibrated mixture, two-dimensional NMR analysis of D-mannose and D-fructose in the sample was performed. The signals from 2-H of D-mannose and 1-H of β-D-fructopyranose and β-D-fructofuranose were clearly detected in the HSQC analysis (Fig. 4B and C), despite the reaction being performed in D_2O. Thus, these protons were not substituted with deuterium from the reaction solvent upon isomerization.

3.4. Structural analysis of Marme_2490

The structure of Marme_2490 was determined at 2.6 Å resolution (Fig. 5A, Table 3). The overall structure of Marme_2490 is nearly identical to that of a putative AGE from *Xylella fastidiosa* (*Xf*AGE, PDB ID: 3GT5) with a root mean square deviation (RMSD) of 0.75 Å for 386 superimposed Cα atoms, and contains a typical $(\alpha/\alpha)_6$-barrel domain. Two molecules were observed in the asymmetric unit (molecule-A and molecule-B). The structures of these two molecules were almost identical (RMSD for all Cα atoms was 0.26 Å). Since the electron density of molecule-B was seen more clearly than that of molecule-A (residues Asp232–Arg243 of the α7→α8 loop, connecting the 7th and 8th α-helices, of molecule-A were disorder), we describe the structure based on molecule-B. The molecular mass of Marme_2490 under nondenaturing conditions was determined to be about 42 kDa by gel filtration column chromatography (Fig. 5). This molecular mass was close to the calculated molecular mass of the monomeric protein from the amino acid sequence (48.8 kDa), and thus, Marme_2490 was a

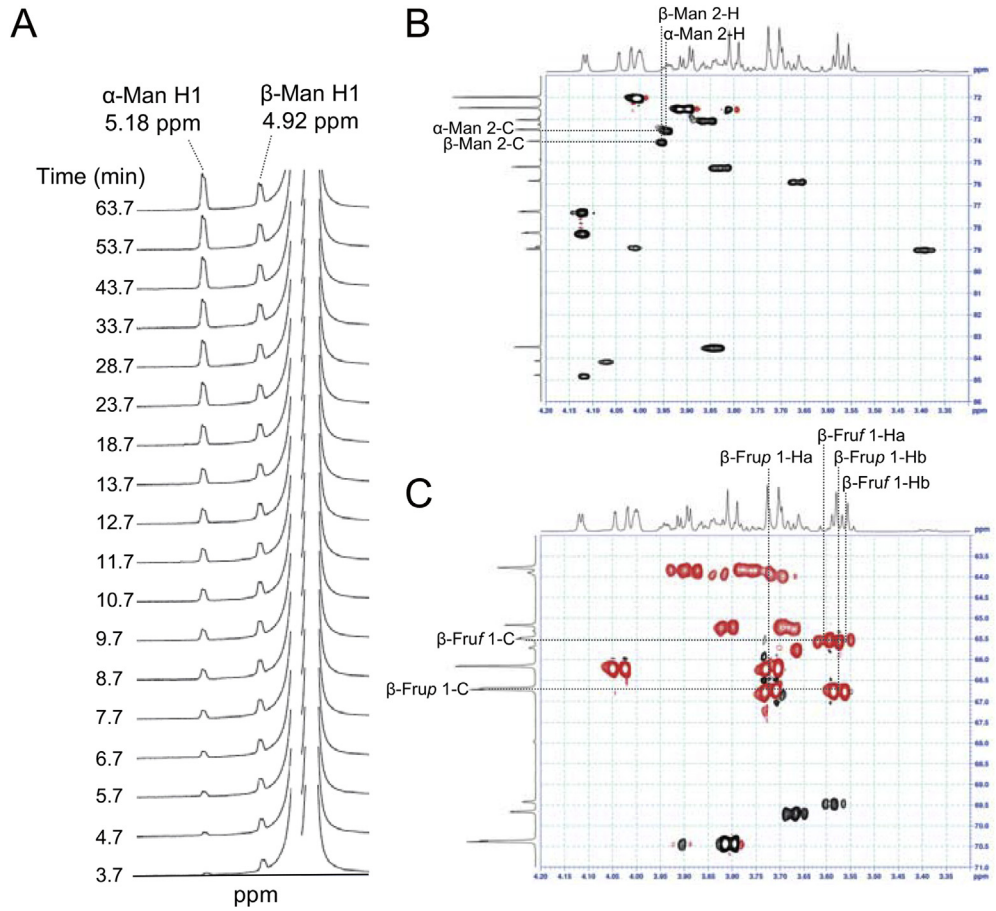

Fig. 4. NMR analysis of the reaction product of Marme_2490. (A) Time course of isomerization of D-fructose. ^{1}H-NMR of the reaction mixture of Marme_2490 with D-fructose was recorded. (B and C) Regions of the HSQC spectrum showing the signals arising from the equilibrated reaction product of Marme_2490. The correlation signals of 2-C and 2-H of D-mannose and 1-C and 1-H of D-fructose are shown in panels B and C, respectively. Correlation peaks of the methylene groups are shown in red.

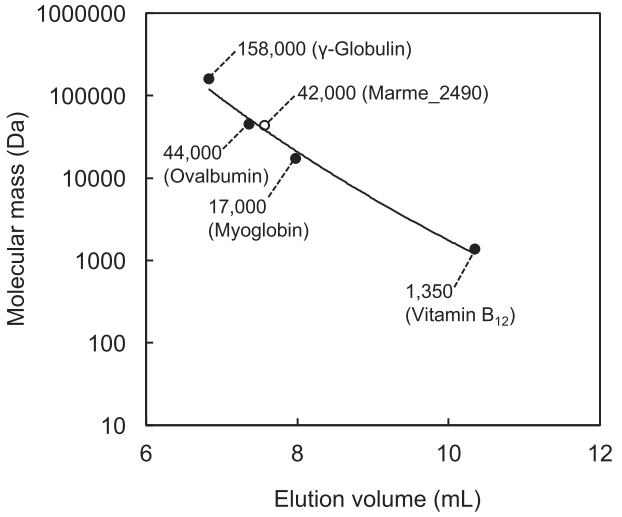

Fig. 5. Estimation of molecular mass of Marme_2490 by gel-filtration column chromatography. Closed and open symbols indicate standard proteins and Marme_2490, respectively.

Table 3
Summary of crystallization conditions, data collection and refinement statistics.

	Marme_2490
PDB ID	5X32
Data collection	
Beamline	SPring-8 BL44XU
Space group	*I*222
Unit cell parameters *a*, *b*, *c*, (Å)	98.9, 100.9, 192.5
Wavelength (Å)	0.9
Resolution range (Å)	50.0–2.6 (2.68–2.6)
R_{meas} (%)*	14.7 (87.1)
<I/s(I)>	10.0 (2.6)
Completeness (%)	99.3 (96.5)
Redundancy	7.4 (7.4)
Refinement	
No. reflection	30,329
R_{work}/R_{free} (%)**	19.4/26.0
No. of atoms	
Macromolecules	6389
Ligand/ion	10
Water	17
B-factors (Å^2)	
Macromolecules	60.6
Ligand/ion	71.5
Water	56.5
Estimated coordinate error	0.38
Rmsd from ideal	
Bond lengths (Å)	0.008
Bond angles (°)	1.24

Values in parentheses are for the highest resolution shell. *$R_{meas} = \Sigma_{hkl}\ \{N(hkl)/[N(hkl) - 1]\}^{1/2}\ \Sigma_i\ |\ I_i(hkl) - <I(hkl)>\ |/\Sigma_{hkl}\ \Sigma_i\ I_i(hkl)$, where $<I(hkl)>$ and $N(hkl)$ are the mean intensity of a set of equivalent reflections and the multiplicity, respectively. **$R_{work} = \Sigma_{hkl}\ ||F_{obs}| - |F_{calc}||/\Sigma_{hkl}\ |F_{obs}|$, R_{free} was calculated for 5% randomly selected test sets that were not used in the refinement.

monomer in solution.

In the structure, a phosphate molecule, which is presumably captured from the crystallization buffer, was observed at the catalytic center (Fig. 6A). All the oxygens of the phosphate were coordinated by surrounding residues which are predicted to be involved in substrate binding. Superimposition of Marme_2490 and the complex of SeAKI with D-mannose (H248A mutant; PDB ID: 2ZBL) suggested that two oxygen atoms of the phosphate were positioned at the equivalent positions of 1-O and 5-O of D-mannose. Inorganic phosphate inhibited the D-mannose isomerization of Marme_2490 through a competitive inhibition process, because the lines obtained from the reaction rates in the absence and presence of inorganic phosphate crossed on the *y*-axis in the Lineweaver-Burk (double-reciprocal) plots (Fig. 7). The K_i value was determined to be 31.5 ± 1.4 mM.

The structure of Marme_2490 was superimposed well onto SeAKI in both the substrate-free form (PDB ID: 2AFA) and the complex with D-mannose (H248A) [11] (Fig. 6B). The orientation of the side chain of His251 of Marme_2490 was similar to that of catalytic His248 of SeAKI in the apo-form, indicating that His251 of Marme_2490 is the catalytic residue. The orientations of Arg57, Asn174, His178, Glu254, Trp312, and His380 of Marme_2490 are also almost identical with corresponding residues of SeAKI, which are involved in the substrate binding. MI and CE catalyze reactions differently from each other, but no obvious structural differences were found in the catalytic sites of Marme_2490 and *Rhodothermus marinus* CE (RmCE) in substrate-free (PDB ID: 3WKF) conditions and in complex with Glcβ1-4Man (PDB ID 3WKG; Fig. 6C) [15].

4. Discussion

Carbohydrate isomerases and epimerases have important functions in various carbohydrate metabolisms, and are useful in industrial carbohydrate enzymatic conversions. MI, a member of the AGE superfamily, is an attractive enzyme that produces D-mannose from inexpensive D-fructose. In this study, Marme_2490, registered as an AGE in the sequence database and showing low sequence similarity with any known enzymes, was shown to not epimerize *N*-acetyl-D-glucosamine, but instead isomerizes D-mannose as the primary substrate.

The amino acid sequence of Marme_2490 is 53.8%–62.4% identical to uncharacterized orthologues from *Marinomonas*, *Pseudomanas*, *Xanthomonas* and *Xylella* species: *Marinomonas posidonica* Mar181_2063 (GenBank ID, AEF55101.1), *Marinomonas profundimaris* D104_03355 (GenBank ID, ETI61935.1), *Marinomonas ushuaiensis* MUS1_08255 (GenBank ID, ETX11921.1), *Pseudomonas luteoviolacea* JF50_16005, (GenBank ID, KID55850.1), *Pseudomonas oryzihabitans* APT59_12760 (GenBank ID, ALZ85017.1), *Pseudomonas psychrotolerans* NS337_14990 (GenBank ID, KTT52847.1), *Xanthomonas axonopodis* XAXN_18570 (GenBank ID, KPL47648.1), and *Xylella fastidiosa* RA12_07325 (GenBank ID, KIA58312.1). No genes predicted to be involved in carbohydrate metabolism were present in the neighboring genes of *Marme_2490*, but the putative fructokinase genes, *JF50-16000* of *P. luteoviolacea* (GenBank number, KID55849.1) and *RA12_07320* of *X. fastidiosa* (GenBank number, KIA58311.1) were present. This implied that these orthologues isomerized D-mannose to D-fructose. D-Fructose produced was presumed to be phosphorylated by the fructokinase and metabolized through the Embden-Meyerhof-Parnas pathway. The putative fructokinase gene (Marme_4041; GenBank number, ADZ93249.1) was also present in the *M. mediterranea* genome, and thus, Marme_2490 was likely involved in D-mannose metabolism together with the fructokinase.

In the kinetic analysis of D-mannose isomerization (Table 2), Marme_2490 showed 2.9–113-fold higher k_{cat}/K_m than those of *E. coli* AKI (EcAKI), SeAKI, and TfMI, even though the kinetic analysis of Marme_2490 was conducted at a lower temperature (30 °C) than the compared enzymes (37–50 °C). Among these four enzymes, the k_{cat}/K_m values of EcAKI and SeAKI for D-mannose were considerably low, although Itoh et al. have reported that D-mannose was the best substrate of these enzymes among tested substrates [11]. Recently, the isomerization activity of EcAKI to sulphoquinovose (6-deoxy-6-sulphoglucose) to 6-deoxy-6-sulphofructose was described [27], and EcAKI might use sulphoquionvose as a better substrate than D-

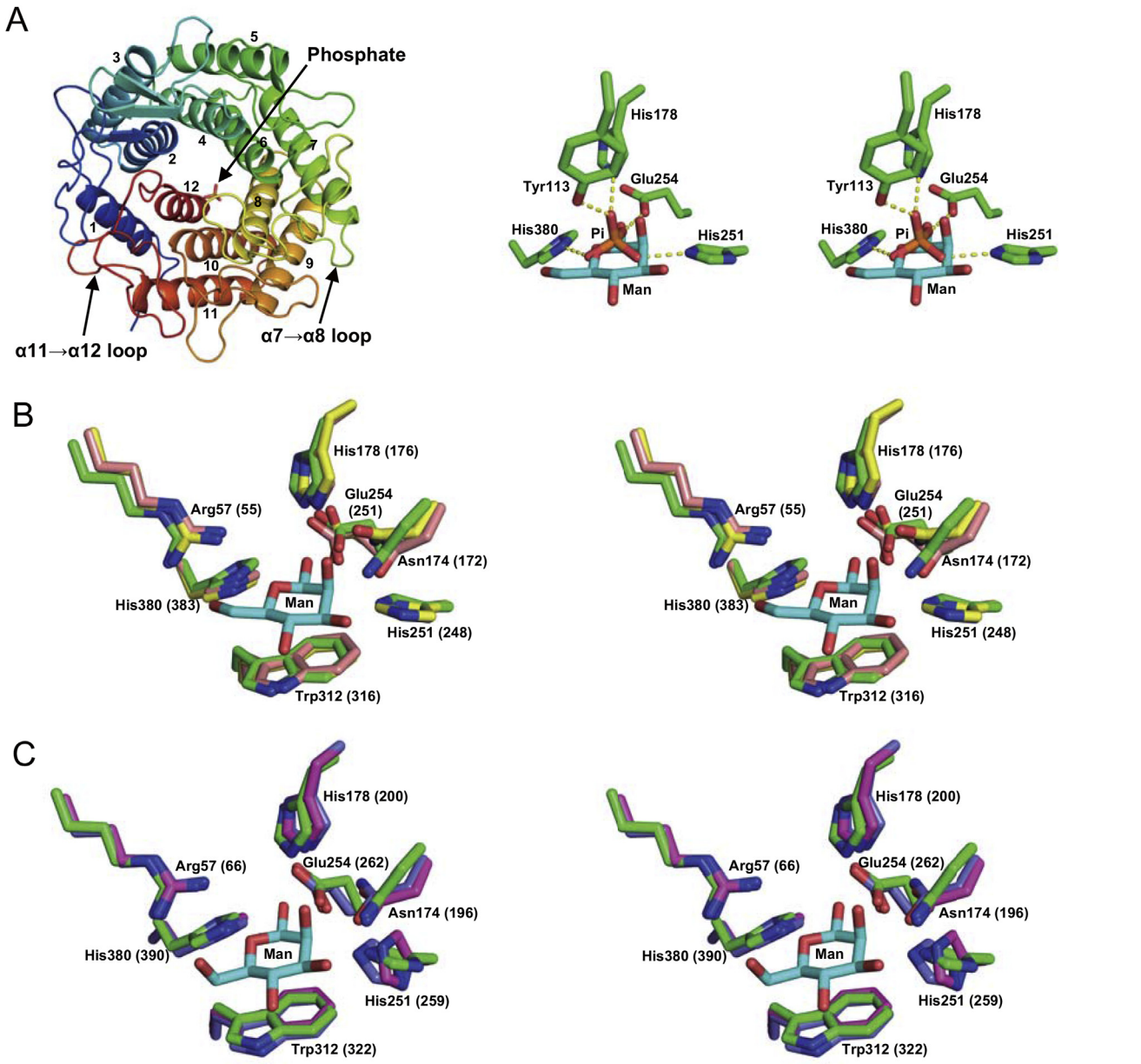

Fig. 6. Structure of Marme_2490. (A) Cartoon model of Marme_2490 with the phosphate shown as a stick model. The overall structure is shown in rainbow coloring from N-terminus (blue) to C-terminus (red) (left panel). Interactions between the phosphate and surrounding amino acid residues are shown in the right panel. Predicted hydrogen bonds are shown as yellow dashed lines. D-Mannose bound to SeAKI H248A is superimposed. (B) Superimposition of structures of Marme_2490 (green) and SeAKI in the substrate-free form (wild-type, yellow) and in complex with D-mannose (H248A, pale orange). D-Mannose is shown in cyan. Amino acid numbers of SeAKI are shown in parenthesis. (C) Superimposition of structures of Marme_2490 (green) and RmCE in the substrate-free form (blue) and in complex with Glcβ1-4Man (magenta). The reducing end D-mannose residue is shown in cyan. Amino acid numbers of RmCE are shown in parenthesis.

mannose.

MI and AKI are distinguishable based on their isomerization activities for D-glucose: AKI has a weak but apparent D-glucose isomerizing activity [11], while MI does not [5,6,9]. The isomerization activity of Marme_2490 toward D-glucose was not detectable in substrate screening, which clearly indicated that Marme_2490 was not an AKI but an MI. As D-xylose was also not isomerized by Marme_2490, the axial OH group at the D-aldose 2-C position was essential for the catalytic activity of Marme_2490.

Marme_2490 possessed isomerization activity for D-lyxose, as has been observed in other D-mannose-isomerizing enzymes, such as MIs and AKIs [6,9,11]. In the complex of SeAKI and D-mannose [11], the D-mannose 6-OH forms hydrogen bond with Arg55, which is highly conserved in AGE superfamily members. The activity of MIs and AKIs to D-lyxose indicated that this interaction was not essential for catalysis.

In addition to isomerization activities to D-mannose and D-lyxose, Marme_2490 isomerized 4-OH derivatives of D-mannose, D-talose, and β-(1→4)-disaccharides. Isomerization activity for these sugars was first reported in Marme_2490 and is useful as a biocatalyst for carbohydrate conversions.

The structural basis for Marme_2490's substrate specificity was addressed by comparing the structure of Marme_2490 in free form with SeAKI and RmCE. In SeAKI, the orientations of its α7→α8 and

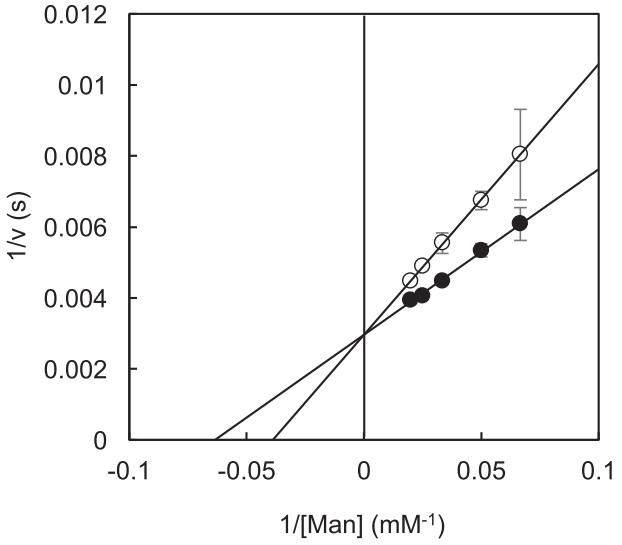

Fig. 7. Lineweaver-Burk plots of Marme_2490 isomerization of D-mannose in the absence and presence of inorganic phosphate. Reaction rates at indicated concentrations of D-mannose in the absence (closed circles) and presence (open circles) of 20 mM inorganic phosphate are shown. Values are the average of three independent experiments, and error bars show the standard deviation of the three values.

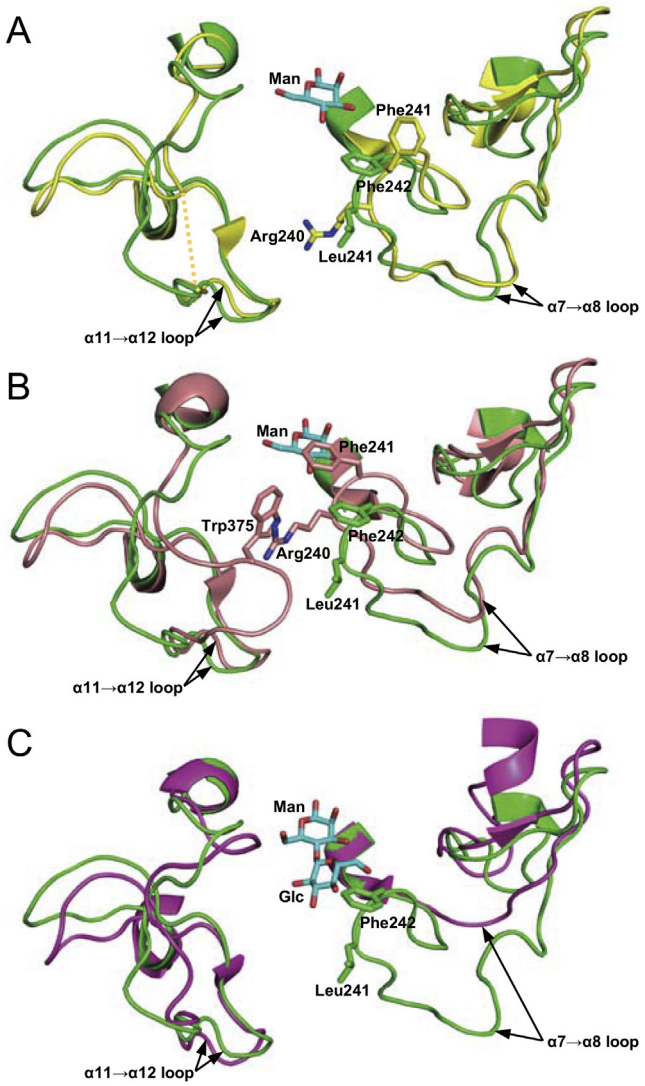

Fig. 8. Structural comparison of Marme_2490 with SeAKI and RmCE. (A) Comparison of structures of α7→α8 and α11→α12 loops of Marme_2490 (green) and SeAKI in the apo-form (yellow). The α11→α12 loop of SeAKI is invisible (broken line). D-Mannose (cyan) bound to SeAKI H248A is superimposed. (B) Comparison of structures of α7→α8 and α11→α12 loops of Marme_2490 (green) and SeAKI H248 in complex with D-mannose (pale orange). D-Mannose is shown in cyan. (C) Comparison of structures of α7→α8 and α11→α12 loops of Marme_2490 (green) and RmCE in complex with Glcβ1-4Man (magenta). Glcβ1-4Man is shown in cyan.

α11→α12 loops are different in the substrate-free form and the complex with D-mannose (Fig. 8A and B) [11]. The α7→α8 loop of SeAKI is distal from the substrate-binding site in the substrate-free form, but is situated near the D-mannose substrate in the complex. Phe241 in this loop is in close proximity to the 4-C, 5-C, and 6-C of D-mannose, and is predicted to cause severe steric hindrance when the enzyme binds a disaccharide-substrate (Fig. 8B). Consistent with this prediction, the α7→α8 loop of a disaccharide-acting CE is clearly shorter than in monosaccharide specific enzymes and contributes to the formation of an open substrate-binding site to accommodate disaccharide substrates (Fig. 8C) [15]. The SeAKI α11→α12 loop is disordered in the apo-form (Fig. 8A), but is ordered when complexed with D-mannose (Fig. 8B). The Trp375 in this loop forms a hydrophobic interaction with the D-mannose 6-C and the Arg240 side chain in the α7→α8 loop (Fig. 8B). These loops close the substrate-binding site entrance in the D-mannose complex.

The α7→α8 loop of Marme_2490 in the apo-form also adopted an open-form, as has been observed in the apo-form of SeAKI (Fig. 8A) [11]. As this loop in molecule-A of Marme_2490 was disordered (see above), this loop was hypothesized to be more flexible than the same loop in SeAKI. The α7→α8 loop of Marme_2490 contained Phe242, corresponding to SeAKI Phe241 but had a Leu241 at the corresponding position of SeAKI Arg240. The α11→α12 loop of Marme_2490 was ordered even in the substrate-free form and assumed an open-orientation similar to that of RmCE (Fig. 8C). In addition, the enzyme did not contain Trp corresponding to Trp375 of SeAKI. Therefore, the α7→α8 and α11→α12 loops of Marme_2490 were hypothesized not to interact with each other. The entrance of Marme_2490's active pocket in the substrate complex was presumably more open than SeAKI, and the open substrate-binding site provided space for binding 4-OH derivatives of D-mannose. TfMI does not have Arg at the corresponding position of Arg240 of SeAKI (Pro241) but has Trp375 corresponding to Trp375 of SeAKI.

The isomerization mechanism of Marme_2490 was examined and discussed by NMR analysis of the anomeric configuration of D-mannose from D-fructose in the initial reaction and the presence of deuterium in D-mannose and D-fructose in the equilibrated reaction mixture. In the initial reaction, the signal of the β-D-mannose 1-H was more strongly detected than that of α-D-mannose generated, indicating that Marme_2490 produce β-D-mannose from D-fructose. Gradual formation of α-D-mannose observed in the later reaction was presumably because of nonenzymatic mutarotation. The anomeric configuration of the reaction product by Marme_2490 was consistent with ligands bound to SeAKI and RmCE [11,15]. As lactose and cellobiose in the formation of the complexes of wild-type RmCE are epimerized in crystals [15], D-mannose residues in the RmCE complex are considered the product form. Marme_2490 presumably formed β-D-mannose through a ring closure process, in a manner postulated for SeAKI and RmCE [11,15].

In NMR analysis of equilibrated reaction products, the signals of protons at the D-mannose 2-C and D-fructose 1-C were clearly

detected, which suggested that the proton abstracted from D-fructose was not substituted with deuterium from D_2O solvent. This was essentially different from the proton abstraction/addition mechanism postulated in CE and AGE [13,15]. MI is thought to abstract the proton from 1-C of D-fructose to form the *cis*-enediolate intermediate and add the 2-C proton of the intermediate to produce D-mannose. This mechanism in D-fructose isomerization was also postulated based on the structure of SeAKI [11]. The His conserved at the N-terminus of the 8th α-helix of the catalytic domain (His251 in Marme_2490 and His248 in SeAKI) was predicted to act as a general base and acid catalyst (Fig. 1A).

In D-fructose isomerization, deprotonation of 1-O and protonation of 2-O are also required (Fig. 1A), but their mechanisms remain unclear. The essential His residue in the 6th α-helix (His176 in SeAKI) is predicted to form hydrogen bonds with both 1-OH and 2-OH of D-mannose [11] (Fig. 6B), and might transfer the proton from 1-O to 2-O in D-mannose formation. This His is invariant not only in AKI and MI but also in CE. In *Ruminococcus albus* CE, His184 has been shown to be essential for epimerization activity [14], and the His in the 6th α-helix is essential for catalysis of both the isomerase and epimerase reactions (e.g., stabilization of *cis*-enediolate intermediates through hydrogen-bonding interactions). The proton transfer from 1-O to 2-O, which is not mediated by enzyme amino acid residues, might be possible in MI, because no residues are thought to be required for the proton transfer in the reaction of phosphoglucose isomerase (EC 5.3.1.9) [28].

MI and CE catalyze different reactions, but the superimposition of the Marme_2490 structure on RmCE structures showed only slight differences in the orientations of amino acid residues involved in catalysis and substrate binding (Fig. 6C). Thus, the molecular mechanism determining the reaction specificity of AGE superfamily enzymes was unable to be explained by our present knowledge. Further structural and functional analyses of AGE superfamily enzymes are necessary to understand the molecular basis for their reaction specificity.

Author contributions

WS, planned and performed experiments, analyzed data, and wrote the paper; NJ, performed experiments; KK, performed experiments, analyzed data and wrote the paper; YT, performed experiments; MY, analyzed data; HM, analyzed data.

Databases

The atomic coordinates and structure factors (code 5X32) have been deposited in the Protein Data Bank (http://wwpdb.org/).

Conflicts of interest

The authors declare that there is no conflict of interest.

Acknowledgements

We thank Dr. Eri Fukushi from the GC-MS & NMR Laboratory, Research Faculty of Agriculture, Hokkaido University for NMR data analysis, and Ms. Nozomi Takeda and Mr. Tomohiro Hirose of the Global Facility Center, Hokkaido University for the amino acid and MS analyses. We thank the staff of the beamline BL44XU (proposal No. 2016A6611 and 2017A6713) at SPring-8 for their assistance during data collection. This work was supported in part by the Platform for Drug Discovery, Informatics and Structural Life Science from the Ministry of Education, Culture, Sports, Science and Technology, Japan. Part of this study was supported by a Grant-in-Aid for Young Scientists from the Ministry of Education, Culture, Sports, Science, and Technology of Japan [grant number 26850059] and Young Investigator Research Grants of the Noda Institute for Scientific Research.

References

[1] S.H. Bhosale, M.B. Rao, V.V. Deshpande, Molecular and industrial aspects of glucose isomerase, Microbiol. Rev. 60 (1996) 280–300.
[2] M. Kuyper, A.A. Winkler, J.P. van Dijken, J.T. Pronk, Minimal metabolic engineering of *Saccharomyces cerevisiae* for efficient anaerobic xylose fermentation: a proof of principle, FEMS Yeast Res. 4 (2004) 655–664.
[3] W. Saburi, T. Yamamoto, H. Taguchi, S. Hamada, H. Matsui, Practical preparation of epilactose produced with cellobiose 2-epimerase from *Ruminococcus albus* NE1, Biosci. Biotechnol. Biochem. 74 (2010) 1736–1737.
[4] K. Takeshita, A. Suga, G. Takada, K. Izumori, Mass production of d-psicose from d-fructose by a continuous bioreactor system using immobilized d-tagatose 3-epimerase, J. Biosci. Bioeng. 90 (2000) 453–455.
[5] N.J. Palleroni, M. Doudoroff, Mannose isomerase of Pseudomonas saccharophila, J. Biol. Chem. 218 (1956) 535–548.
[6] J. Hirose, K. Maeda, H. Yokoi, Y. Takasaki, Purification and characterization of mannose isomerase from *Agrobacterium radiobacter* M-1, Biosci. Biotechnol. Biochem. 65 (2001) 658–661.
[7] A. Hey-Ferguson, A.D. Elbein, Purification of a d-mannose isomerase from Mycobacterium smegmatis, J. Bacteriol. 101 (1970) 777–780.
[8] P. Allenza, M.J. Morrell, R.W. Detroy, Conversion of mannose to fructose by immobilized mannose isomerase from Pseudomonas cepacia, Appl. Biochem. Biotechnol. 24 (1990) 171–182.
[9] T. Kasumi, S. Mori, S. Kaneko, H. Matsumoto, Y. Kobayashi, Y. Koyama, Characterization of mannose isomerase from a cellulolytic actinobacteria *Thermobifida fusca* MBL10003, J. Appl. Glycosci. 61 (2014) 21–25.
[10] Y. Takasaki, S. Takano, O. Tanabe, Studied on the isomerization of sugars by bacteria. Part VIII. Purification and some properties of mannose isomerase from *Xanthomonas rubrilineans* S-48, Agric. Biol. Chem. 28 (1964) 605–609.
[11] T. Itoh, B. Mikami, W. Hashimoto, K. Murata, Crystal structure of YihS in complex with d-mannose: structural annotation of *Escherichia coli* and *Salmonella enterica* yihS-encoded proteins to an aldose-ketose isomerase, J. Mol. Biol. 377 (2008) 1443–1459.
[12] T. Itoh, B. Mikami, I. Maru, Y. Ohta, W. Hashimoto, K. Murata, Crystal structure of *N*-acyl-d-glucosamine 2-epimerase from porcine kidney at 2.0 Å resolution, J. Mol. Biol. 303 (2000) 733–744.
[13] Y.C. Lee, H.M. Wu, Y.N. Chang, W.C. Wang, W.H. Hsu, The central cavity from the $(\alpha/\alpha)_6$ barrel structure of *Anabaena* sp. CH1 *N*-acetyl-d-glucosamine 2-epimerase contains two key histidine residues for reversible conversion, J. Mol. Biol. 367 (2007) 895–908.
[14] T. Fujiwara, W. Saburi, S. Inoue, H. Mori, H. Matsui, I. Tanaka, M. Yao, Crystal structure of *Ruminococcus albus* cellobiose 2-epimerase: structural insights into epimerization of unmodified sugar, FEBS Lett. 587 (2013) 840–846.
[15] T. Fujiwara, W. Saburi, H. Matsui, H. Mori, M. Yao, Structural insights into the epimerization of β-1,4-linked oligosaccharides catalyzed by cellobiose 2-epimerase, the sole enzyme epimerizing non-anomeric hydroxyl groups of unmodified sugars, J. Biol. Chem. 289 (2014) 3405–3415.
[16] S. Moore, W.H. Stein, Photometric ninhydrin method for use in the chromatography of amino acids, J. Biol. Chem. 176 (1948) 367–388.
[17] R. Kawahara, W. Saburi, R. Odaka, H. Taguchi, S. Ito, H. Mori, H. Matsui, Metabolic mechanism of mannan in a ruminal bacterium, *Ruminococcus albus*, involving two mannoside phosphorylases and cellobiose 2-epimerase: discovery of a new carbohydrate phosphorylase, β-1,4-mannooligosaccharide phosphorylase, J. Biol. Chem. 287 (2012) 42389–42399.
[18] K. Hamura, W. Saburi, H. Matsui, H. Mori, Modulation of acceptor specificity of *Ruminococcus albus* cellobiose phosphorylase through site-directed mutagenesis, Carbohydr. Res. 379 (2013) 21–25.
[19] P.E. Preffer, K.B. Hicks, Characterization of keto disaccharides in solution by deuterium-induced, differential isotope-shift ^{13}C-N.M.R. spectroscopy, Carbohydr. Res. 102 (1982) 11–22.
[20] R.G. Kulka, Colorimetric estimation of ketopentoses and ketohexoses, Biochem. J. 63 (1956) 542–547.
[21] W. Kabsch, XDS, Acta Crystallogr. D. Biol. Crystallogr. 66 (2010) 125–132.
[22] B.W. Matthews, Solvent content of protein crystals, J. Mol. Biol. 33 (1968) 491–497.
[23] P.D. Adams, P.V. Afonine, G. Bunkoczi, V.B. Chen, I.W. Davis, N. Echols, J.J. Headd, L.W. Hung, G.J. Kapral, R.W. Grosse-Kunstleve, A.J. McCoy, N.W. Moriarty, R. Oeffner, R.J. Read, D.C. Richardson, J.S. Richardson, T.C. Terwilliger, P.H. Zwart, PHENIX: a comprehensive Python-based system for macromolecular structure solution, Acta Crystallogr. D. Biol. Crystallogr. 66 (2010) 213–221.
[24] A.J. McCoy, R.W. Grosse-Kunstleve, P.D. Adams, M.D. Winn, L.C. Storoni, R.J. Read, Phaser crystallographic software, J. Appl. Cryst. 40 (2007) 658–674.
[25] P. Emsley, K. Cowtan, Coot: model-building tools for molecular graphics, Acta Crystallogr. D. Biol. Crystallogr. 60 (2004) 2126–2132.
[26] V.B. Chen, W.B. Arendall, J.J. Headd, D.A. Keedy, R.M. Immormino, G.J. Kapral, L.W. Murray, J.S. Richardson, D.C. Richardson, MolProbity: all-atom structure validation for macromolecular crystallography, Acta Crystallogr. D. Biol. Crystallogr. 66 (2010) 12–21.

[27] K. Denger, M. Weiss, A.K. Felux, A. Schneider, C. Maver, D. Spiteller, T. Huhn, A.M. Cook, D. Schleheck, Sulphoglycolysis in *Escherichia coli* K-12 closes a gap in the biogeochemical sulphur cycle, Nature 507 (2014) 114–117.

[28] D. Arsenieva, R. Hardré, L. Salmon, C.J. Jeffery, The crystal structure of rabbit phosphoglucose isomerase complexed with 5-phospho-d-arabinonohydroxamic acid, Proc. Natl. Acad. Sci. U. S. A. 99 (2002) 5872–5877.